### CHAPTER 55

# OSCILLATORY BOTTOM BOUNDARY LAYER BY LOW-REYNOLDS NUMBER

### TURBULENCE MODEL

TOSHIYUKI ASANO1)

HITOMI GODO<sup>2</sup>)

YUICHI IWAGAKI3)

#### ABSTRACT

Characteristics of mean velocity and turbulence properties in oscillatory bottom boundary layers are investigated with low-Reynolds number turbulence model. Since this model is capable to describe the flow field close to the bottom, special attentions are paid on the characteristics of the viscous sublayer. Several interesting results, which coincide with or differ from existing knowledge on steady bottom boundary layers, are presented in paticular on the mean velocity profile, turbulent viscosity coefficient and growth of the viscous sublayer.

# I. INTRODUCTION

Existing studies for turbulent transport phenomena in coastal processes are mainly based on the eddy viscosity concept. However, it has been recognized that the predictive ability of eddy viscosity models is severely limited. Recently, as the computer technology has been advancing, applications of turbulent transport models to oscillatory flow have received special interest. At present, k- $\epsilon$  model is regarded as the most widely tested and the most applicable two equation model, in which two partial differencial equations are used to describe turbulent kinematic energy k and its dissipation rate  $\epsilon$ .

A few researchers have investigated the applicability of the  $k-\epsilon$  model to oscillatory boundary layers (Cousteix et al.,1979; Hayashi and Shinoda, 1979; Shen, 1984) , most of these studies dealing only with a high Reynold number version of the  $k-\epsilon$  model. Such a model is no longer applicable to the near bottom region, where the local isotropic condition is not satisfied. Besides, in oscillatory flow, the velocity is so small when the flow direction changes that the turbulence is not always intensive throughout a full period. From above reasons, a  $k-\epsilon$  model which accounts for low-Reynolds number effects should be applied to oscillatory turbulent boundary layers.

<sup>1)</sup> Dr. Eng., Research Associate, Dept. of Civil Eng., Kyoto Univ. Sakyo-ku, Kyoto, 606, JAPAN

<sup>2)</sup> M. Eng., Ministry of Construction (Formerly Post-graduate Student, Kyoto Univ.), JAPAN

<sup>3)</sup> Dr. Eng., Professor, Dept. of Civil Eng., Meijo Univ., Tenpaku-ku, Nagoya, 468, JAPAN

This study examines the applicability of a  $k-\epsilon$  model of low-Reynolds number version to oscillatory boundary layers. From the results obtained, characteristics of both the mean velocity and turbulence are discussed. Furthermore, since the model describes the flow field close to the bottom, comprehensive investigations have been made on the characteristics of the viscous sublayer. The growth of the viscous sublayer under the flow acceleration is investigated in relation to a phenomenon of 're-laminarization' in an accelerated uni-directional flow.

# II. k-& MODEL FOR LOW-REYNOLDS NUMBERS

In order to predict the flow within a viscous sublayer close to the bottom, Jones and Launder (1972,a) have introduced the following extra terms into the standard  $k-\epsilon$  model: (1) terms to represent viscous diffusion of k and  $\epsilon$ , and (2) terms to account for the non-isotropic dissipation process. Furthermore, they have modified some coefficients in the  $k-\epsilon$  equations into functions of the turbulence Reynolds number  $R_T$ , which is defined with  $k,\ \epsilon$  and kinematic viscosity  $\nu$  as follows:

$$R_T = k^2 / \nu \epsilon \tag{1}$$

For a steady flow, the wall function method (Rodi, 1978) is often used as an alternative to the direct consideration of viscous sublayer properties. In this method the boundary conditions at the bottom are replaced by those immediately outside the viscous sublayer based on empirical laws under the local turbulence equilibrium condition. The method, however, is not applicable to an oscillatory flow since the rate of turbulence generation does not coincide with that of its dissipation at each phase. One of the merits of the low-Reynolds number  $k_{-\ell}$  model is that all the variables at the bottom can be set to be zero without invoking any empirical knowledge.

### III OUTLINE OF THE ANALYSIS

### (1) Basic equations

The oscillatory boundary layer equation is given as follows:

$$\frac{\partial (u - u_p)}{\partial t} = -\frac{\overline{\partial u'w'}}{\partial z} + \nu \frac{\partial^2 u}{\partial z^2}$$
 (2)

where x and z axes are taken along and normal to the flat bottom respectively, t is the time, u is the mean velocity in the boundary layer, up is the mean velocity at the outer edge of the boundary layer, and u' and w' are the fluctuating velocity components. The Reynolds stress  $-\rho \overline{\mathbf{u}^{\mathsf{i}}\mathbf{w}^{\mathsf{i}}}$  is expressed as a product of mean rate of strain  $\partial \mathbf{u}/\partial z$  and turbulent viscosity  $\nu_{\mathrm{T}}$ .

$$-\overline{u'w'} = v_T \frac{\partial u}{\partial z} \tag{3}$$

The turbulent viscosity  $\nu_{\rm T}$  is determined by local values of turbulent kinematic energy k and its dissipation rate  $\epsilon$ .

$$\nu_T = c_\mu f_\mu k^2 / \varepsilon \tag{4}$$

According to Jones and Launder's model (1972,a), the following equations are adopted for k and  $\epsilon$ .

$$\frac{\partial k}{\partial t} = \frac{\partial}{\partial z} \left[ \left( \nu + \frac{\nu_T}{\sigma_k} \right) \frac{\partial k}{\partial z} \right] - \overline{u'w'} \frac{\partial u}{\partial z} - \epsilon - 2\nu \left( \frac{\partial k^{1/2}}{\partial z} \right)^2$$
 (5)

$$\frac{\partial \varepsilon}{\partial t} = \frac{\partial}{\partial z} \left\{ \left( \underbrace{v + \frac{v_T}{\sigma_{\varepsilon}}} \right) \frac{\partial \varepsilon}{\partial z} \right\} - c_1 \underbrace{f_1 \frac{\varepsilon}{k} \overline{u'w'}}_{\partial z} \frac{\partial u}{\partial z} - c_2 \underbrace{f_2 \frac{\varepsilon^2}{k}}_{\partial z} + 2vv_T \left( \frac{\partial^2 u}{\partial z^2} \right)^2$$
 (6)

The underlined terms are included to account for low-Reynolds number effects. After Jones and Launder, the coefficients in Eqs.  $(4) \sim (6)$  are given as follows:

$$c_{\mu} = 0.09, \qquad c_{1} = 1.55, \qquad c_{2} = 2.0, \\ \sigma_{k} = 1.0, \qquad \sigma_{s} = 1.3$$
 (7)

The following expressions proposed by Jones and Launder for  $f_1$ ,  $f_2$ ,  $f_\mu$  are also adopted.

$$f_1 = 1.0 f_2 = 1.0 - 0.3 \exp(-R_7^2) f_2 = \exp\{-2.5/(1 + R_7/50)\}$$
 (8)

These are a lot of arguments (Hanjalic and Launder, 1976; Hosoda and Yokoshi, 1986) concerning the values of the coefficients in Eq. (7) and the functional forms in Eq. (8) even for steady flows. Another problem may arise in applying the values and functional forms proposed for steady flows to oscillatory flows. However, they have been confirmed to be universal at least for various types of steady flow. Furthermore, as seen from Eq.(1), the turbulent Reynolds number  $R_{\rm T}$  varies spatially and temporally with k and  $\epsilon$ , and it is expected that the vaiations of  $f_2$  and  $f_\mu$  express the temporal variations of the oscillatory flow properties.

### (2) Non-dimensional description of basic equations

To obtain non - dimensional forms of the basic equations, the following variables are introduced:

$$\bar{u}_r = (u - u_p)/\hat{u}_p, \quad z_r = z/\delta, \quad t_r = \omega t, 
\tau_r = -u'w'/\hat{u}_p^2 \quad k_r = k/\left(\frac{1}{2}\hat{u}_p^2\right), \quad \varepsilon_r = \varepsilon/\left(\frac{1}{2}\omega\hat{u}_p^2\right)$$
(9)

where  $\widehat{u}_p$  is the velocity amplitude immediately outside the boundary layer,  $\omega$  is the angular frequency of the oscillatory flow,  $\delta = \sqrt{\nu/\omega}$  is related to Stokes length. Now, the system of the equations to be analysed here is as follows:

$$\frac{\partial \tilde{u}_r}{\partial t_r} = R^{1/2} \frac{\partial \tau_r}{\partial z_r} + \frac{\partial^2 \tilde{u}_r}{\partial z_z^2} \tag{10}$$

$$\tau_r = \frac{1}{2} R^{1/2} c_{\mu} f_{\mu} \frac{k_r^2}{\epsilon_r} \frac{\partial \tilde{u}_r}{\partial z_r}$$
 (11)

$$\frac{\partial k_r}{\partial t_r} = \frac{\partial}{\partial z_r} \left\{ \left( 1 + \frac{1}{2} R \frac{c_{\mu}}{\sigma_k} f_{\mu} \frac{k_r^2}{\epsilon_r} \right) \frac{\partial k_r}{\partial z_r} \right\}$$

$$+2R^{1/3}\tau_r\frac{\partial \tilde{u}_r}{\partial z_r} - \varepsilon_r - 2\left(\frac{\partial k_r^{1/2}}{\partial z_r}\right)^2 \tag{12}$$

$$\frac{\partial \varepsilon_r}{\partial t_r} = \frac{\partial}{\partial z_r} \left\{ \left( 1 + \frac{1}{2} R \frac{c_\mu}{\sigma_s} f_\mu \frac{k_r^2}{\varepsilon_r} \right) \frac{\partial \varepsilon_r}{\partial z_r} \right\}$$

$$+2R^{1/2}c_1f_1\frac{\varepsilon_r}{k_r}\tau_r\frac{\partial u_r}{\partial z_r} - c_2f_2\frac{\varepsilon_r^2}{k_r} +2Rc_\rho f_\rho\frac{k_r^2}{\varepsilon_r}\left(\frac{\partial^2 \bar{u}_r}{\partial z_r^2}\right)^2$$
(13)

where R is the Reynolds number defined as follows:

$$R = \left(\frac{\widehat{u}_p}{\omega \delta}\right)^2 = \frac{\widehat{u}_p a}{v}$$
 (14)

where a is the orbital amplitude at the bottom.

By using low Reynolds number  $k-\xi$  model, the bottom boundary condition is described in the following simple way.

$$\tilde{u}_r = -\cos t_r, \quad k_r = 0, \quad \epsilon_r = 0, \quad \text{at } z_r = 0$$
 (15)

The upper boundary condition is described as follows.

$$\frac{\partial \tilde{u}_r}{\partial z_r} = 0, \qquad \frac{\partial k_r}{\partial z_r} = 0, \qquad \frac{\partial \varepsilon_r}{\partial z_r} = 0, \qquad \text{at} \quad z_r = 1$$
 (16)

## (3) Computational Technique

The vertical grid spacing  $\Delta z$  was determined at D/600(D: the height where shear stress becomes negligible) to obtain sufficient number of grid points in the viscous sublayer. The system of the basic equations (10) $\sim$ (13) was solved by the Crank-Nicolson implicit scheme. The time increment  $\Delta t$  was T/2160. The calculation was continued until the variables at a phase in successive cycles converge. The conditions of calculations are listed in Table 1.

Table 1 Conditions of calculations.

	$\widehat{\mathrm{u}}_{\mathrm{p}}$	Т	D	
	(cm/sec)	(sec)	(cm)	R
CASE-I	30.0	9.8	4.0	1.40×10 <sup>5</sup>
CASE-II	30.0	15.0	4.0	2.15×10 <sup>5</sup>
CASE-III	40.0	9.8	5.0	2.50×10 <sup>5</sup>
CASE-IV	49.9	9.8	7.0	3.87×10 <sup>5</sup>
CASE-V	49.9	15.0	7.0	5.93×10 <sup>5</sup>

## IV. RESULTS AND DISCUSSION

## (1) Mean velocity and turbulence properties

Figure 1 shows profiles of the non-dimensional mean velocity  $\mathbf{u_r}$ , Reynolds stress  $r_{\mathbf{r}}$ , turbulent energy  $\mathbf{k_r}$  and its dissipation rate  $\epsilon_{\mathbf{r}}$  for every  $\pi/6$  phase. In Fig.1 and following all figures, the height z is normalized by D  $(\mathbf{z_r'} = \mathbf{z}/D)$  instead of  $\delta$   $(\mathbf{z_r} = \mathbf{z}/\delta)$ . It is found in the results at the phases 0 and  $\pi$  that the heights where the mean velocity reaches its maximum increase with the Reynolds number R; that is, the velocity gradient decreases with R.

Figure 2 depicts variations of these quantities with phase. The peak values of  $\tau_{\Gamma}$ ,  $k_{\Gamma}$  and  $\epsilon_{\Gamma}$  becomes larger as R increases. The phase lags of the maxima of  $\tau_{\Gamma}$ ,  $k_{\Gamma}$  and  $\epsilon_{\Gamma}$  behind the maxima of the outer velocity decrease with increase in R. It should be noted that the phase of the total shear stress  $-\rho u^{\dagger} w^{\dagger} + \rho \nu \partial u / \partial z$  close to the bottom goes ahead of the phase of the outer velocity although the phase of the Reynolds stress  $-\rho u^{\dagger} w^{\dagger} \log z$  behind it.

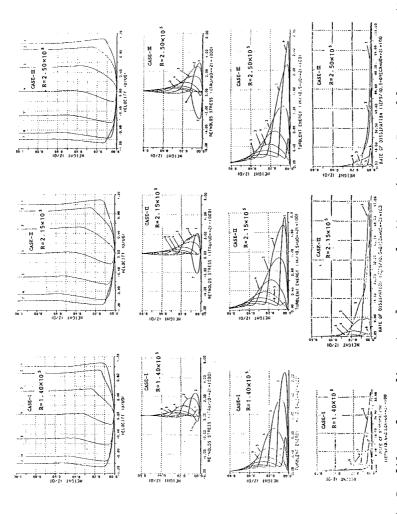
Profiles of the mean velocity  $u_r$  are given in Figure 3, where the ordinate is taken in the logarithmic scale. The figure also shows the positions of the outer edge of the viscous sublayer  $D_L$  and the overlapped layer d estimated on the basis of Kajiura's (1968) theory. It is observed in the profiles around the phase 0 and  $\pi$  that the mean velocity shows linear variation in the region  $z_r'<D_L/D$ , and log-linear variation in the region  $D_L/D<z_r'<d/D$ . These properties are consistent with the general findings in steady unidirectional flow. Such properties however are not so obvious for the other phases.

## (2) Turbulent viscosity coefficient

Figure 4 shows the profiles of the turbulent viscosity coefficient  $\nu_T$  ,which is calculated by the local instantaneous values of k and  $\epsilon$  shown in Eq.(4). It is found that  $\nu_T$  increases almost linearly in the region close to the bottom; the phase averaged value of  $\nu_T$  is almost constant in the region of 0.1<zr'<0.4;  $\nu_T$  decreases with the height in the outer region zr'>0.4.

### (3) Transport process of turbulent energy

Figure 5 shows the turbulent energy balance in the oscillatory boundary layer for CASE-I. The symbols Dif, P,  $\epsilon$  and Ni in the figure denote the turbulence diffusion(1st term of R.H.S. of Eq.(12)), production (2nd term), dissipation(3rd term) and non-isotropic part of the dissipation near the bottom(4th term).



Profiles of non-dimensional mean velocity  $\text{u}_{\Gamma}(\text{top})$  , Reynolds stress  $\tau_{\Gamma}(\text{2nd})$  , turbulent energy  $k_{\mathbf{r}}\left(3rd\right)$  and turbulent energy dissipation rate  $\epsilon_{\mathbf{r}}\left(bottom\right)$  . Fig.1

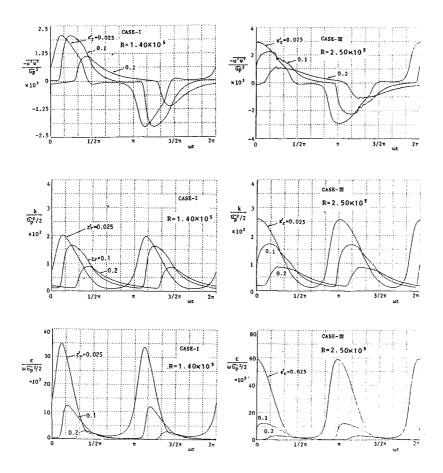


Fig.2 Phase variations of Reynolds stress  $\tau_{\bf r}(\text{top})$ , turbulent energy  $k_{\bf r}(\text{middle})$  and turbulent energy dissipation rate  $\epsilon_{\bf r}(\text{bottom})$ .

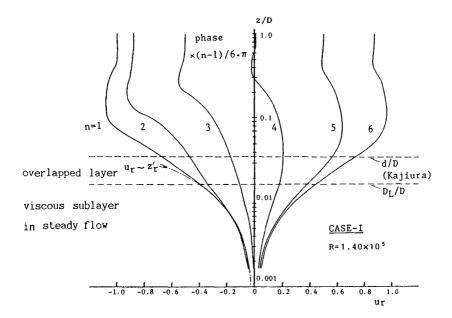


Fig. 3 Profiles of mean velocity.

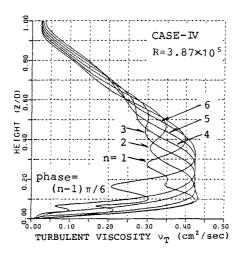


Fig.4 Profiles of turbulent viscosity  $\nu_{\rm T}.$ 

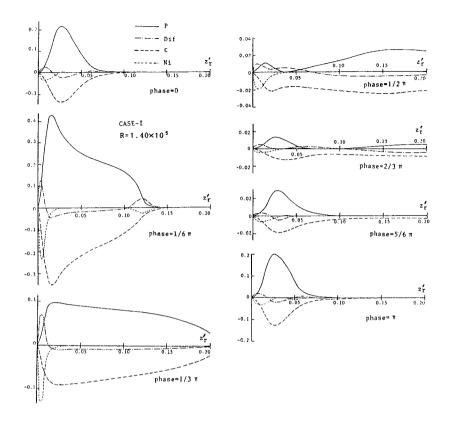


Fig.5 Turbulent energy balance near the bottom.

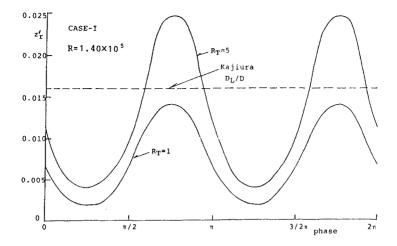


Fig.6 Variations of the height of viscous sublayer with phase.

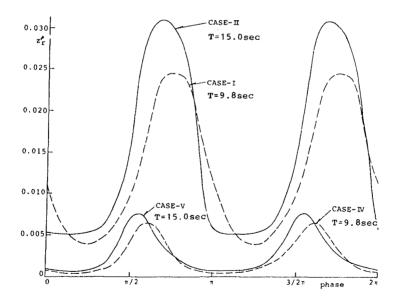


Fig.7 Variations of the height of viscous sublayer with phase (at the height where  $R_{\rm T}\!=\!5)\,.$ 

## (4) Variation of the height of viscous sublayer

In Kajiura's(1968) theory, the height of the viscous sublayer is assumed to be invariant regardless of phase. However, it is found from the following consideration that the height varies with the phase.

varies with the phase. The total shear stress  $\tau_{\rm A}$  consists of the viscous and the turbulent shear stresses.

$$\tau_A = \rho(\nu + \nu_T) \frac{\partial u}{\partial z} \tag{17}$$

From Eqs.(1) and (4),  $\nu_{\rm T}$  is expressed as a function of the turbulent Reynolds number  $R_{\rm T}$ :

$$\nu_T = c_u f_u \nu R_T \tag{18}$$

Consequently, the ratio of the viscous shear stress to the total shear stress is a function of  $R_T.$  The viscous shear stress occupies 95.7% of the total shear stress when  $R_T \!\!=\! 5$ , and 99.2% when  $R_T \!\!=\! 1.$  If the outer edge of the viscous sublayer is defined as a position where  $R_T$  equals 5, the phase averaged height coincides well with that estimated from Kajiura's theory for all cases of the present calculations. The coincidence is not surprising because both this model and Kajiura's theory are based on same experimental knowledge on steady bottom boundary layers.

Figure 6 shows variations of the heights where  $R_{\rm T}$  equals 5 and 1. It is concluded that the thickness of the viscous sublayer varies with the phase and reaches the maximum slightly after the occurrence of the maximum acceleration. In other words, the turbulent energy becomes minimum at the accelerating phases. This is analogious to the re-laminarization in accelerated unidirectional flow(Jones and Launder, 1972b). For an oscillatory pipe flow, Hino et al.(1976) have found experimentally the recovery of a laminar flow condition in the accelarating phases.

Figure 7 shows the variations of the height where  $R_T$  equals 5. Comparisons of cases I and II and of cases IV and V, in which cases the velocity amplitudes are same and the oscillation periods are different, show that the maximum thickness of the viscous sublayer increases as the oscillation period increases. In a steady accelerated flow, the thickness of the viscous sublayer increases with the flow acceleration(Jones and Launder, 1972b), whereas the results in Fig. 7 show the opposite feature that the viscous sublayer becomes thicker under smaller flow acceleration. Such difference is attributed to the time required for turbulent energy decay. In the case of short-period oscillating flow, the duration of small flow velocity is not enough for the turbulent energy to attenuate. It can be concluded that the duration of turbulence decaying is a more predominant factor than the effect of flow acceleration for the growth of the viscous sublayer.

### V. CONCLUSIONS

- 1) The variations of the mean velocity and turbulence quantities depending on the Reynolds number have been investigated. The velocity gradients at the phases 0 and  $\pi$  close to the bottom decrease with the Reynolds number. The phase lags of the turbulence quantities behind the outer velocity decrease with increase in the Reynolds number.
- 2) At the phases around 0 and  $\pi$ , the mean velocity varies in proportion to the height from the bottom in the viscous sublayer and shows the logarithmic variation in the overlapped layer. These are consistent with the general findings in steady flow. However, for the other phases such properties are not so obvious.
- 3) The tubulence viscosity coefficient increases in proportion to the height in the region close to the bottom, then keeps almost constant in the region 0.1<z $_{r}$ '<0.4, and decreases with the height in the outer flow region.
- 4) The thickness of the viscous sublayer varies with phases of an oscillatory flow and becomes maximum when the flow accelerates. The thickness increases with the oscillation period, meanwhile it increases with the flow acceleration in accelerated unidirectional flow.

#### REFERENCES

Cousteix, J., A. Desopper and R. Houdeville (1979): Structure and development of a turbulent boundary layer in an oscillatory external flow, Turbulent Shear flow, Vol. 1, Springer-Verlag, pp.154-171.

Hanjalic, K. and B.E. Launder (1976): Contribution toward a Reynolds-Stress closure for low-Reynolds number turbulence, J. Fluid Mech., Vol.74,pp.593-610.

Hayashi, T. and K. Shinoda (1979): Basic study on the turbulent oscillatory boundary layer, Proc. of 23th Japanese Conf. on Hydraulics, pp.41~48.

Hino, M., M. Sawamoto and S. Takasu (1976): Experiments on transition to turbulence in an oscillatory pipe flow, J. Fluid Mech., Vol.75, Part 2, pp.193-207.

Hoshoda, H. and S. Yokoshi (1986): Representation of the dissipation term of  $\epsilon$ -equation in the case of low turbulent Reynolds number, Proc. of 30th Japanese Conf. on Hydraulics, pp.517-522(in Japanese).

Jones, W. P: and B. E. Launder (1972,a): The prediction of laminarization with a two-equation model of turbulence, J. Heat Mass Transfer, Vol.15, pp.301-314.

Jones, W. P. and B. E. Launder (1972,b): Some properties of sink-flow turbulent boundary layers, J. Fluid Mech., Vol. 56, pp.337-351.

Kajiura, K. (1968) : A model of the bottom boundary layer in water waves, Bull. Earthq. Res. Inst., Vol.46, pp.75-123.

Rodi, W. (1978) : Turbulence models and their application in hydraulics, a state of the art review, Univ. Kurlsruhe, SFB 80/T/127, p.140.

Sheng, Y. P. (1984): A turbulent transport model of coastal processes, Proc. of 19th Inter. Conf. of Coastal Eng., pp.2380-2396.